J Mater Sci (2008) 43:5068–5075
DOI 10.1007/s10853-008-2678-y

INTERFACE SCIENCE

Grain growth in porous two-dimensional nanocrystalline materials

Leonid Klinger · Eugen Rabkin · Lasar S. Shvindlerman · Günter Gottstein

Received: 12 February 2008 / Accepted: 25 April 2008 / Published online: 24 May 2008

Abstract Grain growth in two-dimensional polycrystals with mobile pores at the grain boundary triple junctions is considered. The kinetics of grain and pore growth are determined under the assumption that pore sintering and pore mobility are controlled by grain boundary and surface diffusion, respectively. It is shown that a polycrystal can achieve full density in the course of grain growth only when the initial pore size is below a certain critical value which depends on kinetic parameters, interfacial energies, and initial grain size. Larger pores grow without limits with the growing grains, and the corresponding grain growth exponent depends on kinetic parameters and lies between 2 and 4. It is shown that for a polycrystal with subcritical pores the average grain size increases linearly with time during the initial stages of growth, in agreement with recent experimental data on grain growth in thin Cu films and in bulk nanocrystalline Fe.

Introduction

Many unusual properties of nanocrystalline inorganic materials are determined by the fact that a significant portion of all atoms in these materials are located within the grain boundaries (GBs) where atomic coordination and bonding are different from those in the crystalline bulk [1]. However, keeping the grain size in such materials in the nanometric range is difficult because of the high driving force for grain growth which scales inversely with the grain size. The majority of manufacturing methods of nanocrystalline materials results in some residual porosity localized mainly at the triple and quadruple junctions of the GBs. For example, the maximal density achieved in nanocrystalline Pd obtained by inert gas condensation was about 98.5% of bulk density [1]. Moreover, some porosity at the triple and quadruple junctions can form even in initially pore-free nanocrystals at the beginning of grain growth, since the excess volume of some receding GBs cannot be fully absorbed by their neighbors [2–4]. It is clear that grain growth in such materials is strongly affected by residual porosity and should be treated analogously to the combined densification/grain growth during the late stages of sintering [5–6]. However, the applicability of the models developed in previous studies [5–6] to the grain growth in nanocrystaline materials with residual porosity is questionable. For example, Brook has suggested that at the late stages of sintering grain growth is much faster than the corresponding densification rate and, therefore, the latter can be disregarded. Assuming that the pores control the GB mobility and that grain growth causes the pores to coalesce he arrived at the following growth law:

$$\overline{R}^4 - \overline{R}_0^4 = Kt \tag{1}$$

where $\overline{R}^4$, t, and K are the average grain radius, annealing time, and the temperature-dependent kinetic constant, respectively. The temporal separation of grain growth and densification may make sense for conventional polycrystals with a grain size in the micrometer range, since different kinetic constants determine the pores mobility and their shrinking rate (surface and GB diffusivity, respectively).

L. Klinger · E. Rabkin (✉)
Department of Materials Engineering, Technion-Israel Institute of Technology, Haifa 32000, Israel
e-mail: erabkin@tx.technion.ac.il

L. S. Shvindlerman · G. Gottstein
Institute of Physical Metallurgy and Metal Physics, RWTH Aachen University, Aachen 52056, Germany

L. S. Shvindlerman
Institute of Solid State Physics, Russian Academy of Sciences, Chernogolovka, Moscow district 142432, Russia

However, in nanocrystalline materials where pores are separated at very short distances comparable with the grain size the characteristic diffusion distances are also short, and the rate of densification may become comparable with the rate of grain growth. Indeed, the driving force for GB diffusion flux responsible for the shrinkage of the pores scales with γ_s/rR, where γ_s, r and R are the surface energy, pore radius, and grain radius, respectively. Therefore, the rate of densification continuously increases with decreasing grain and pore size, which should be taken into account in the analysis of grain growth in nanocrystalline materials.

Yan, Cannon, and Chowdhry analyzed the grain growth that occurs simultaneously with densification assuming that the former is controlled either by GB mobility or by the mobility of the pores dragged by GBs [6]. It is known that mobile pores or particles merely renormalize the GB mobility leaving the basic kinetic law and topology of grain growth unchanged, provided their number per unit area of the GBs remains constant during grain growth [7]. However, different kinetic growth laws are expected for a polycrystal in which mobile pores are located in the triple and quadruple junctions, making the grain growth problem equivalent to the one of grain growth in a polycrystal with finite mobility of triple and quadruple junctions [8, 9]. For example, in a polycrystal with triple junctions of low mobility a linear growth law should be observed, and the Von Neumann–Mullins relationship governing the topology of the polycrystalline microstructure also changes [8]. It is clear that in nanocrystals with very small and highly mobile pores located at the GB junctions the drag force due to the pores is comparable with the intrinsic GB self-drag, which is defined as the ratio of migration rate and mobility of a pore-free GB [10]. Therefore, in nanocrystals the problem of grain growth, pore coarsening and densification should be treated in a self-consistent way, since it is not known *a priory* which of the factors mentioned above is controlling the whole process. To our knowledge, no such analysis has been performed so far. In the present work we will analyze simultaneous grain growth/densification in a two-dimensional polycrystal with circular pores located at the triple junctions. Though the analysis presented below is of generic nature and valid for arbitrary initial pore and grain sizes, we will focus the subsequent discussion on nanocrystalline materials exhibiting particularly high rates of pore shrinkage.

The model

Two-dimensional grain growth with mobile pores at triple junctions

We will assume that the pores in a two-dimensional nanocrystalline material are located at all triple junctions and are sufficiently mobile, so that no breakaway of migrating GBs from the pores occurs during grain growth. Let us consider a two-dimensional grain limited by n GBs with identical energy and mobility (see Fig. 1). The normal velocity of the curvature-driven motion of each GB, V_n, can be described by the following equation [11]

$$V_n = -M\gamma\kappa = -M\gamma\frac{\partial\theta}{\partial l},$$

where M, γ and κ are the GB mobility, GB energy, and GB curvature, respectively. θ and l are the slope of the GB and the line element of the GB arc, respectively. Thus, the total area of the grain, S, changes with time according to

$$\frac{dS}{dt} = \oint V_n dl = -M\gamma[2\pi - n\Delta\theta], \tag{2}$$

where $\Delta\theta$ is the angle between two neighboring GBs (see Fig. 1). We will further assume that at all stages of grain growth the pores are much smaller than the grains. In this case, the migration of an individual pore is driven by the imbalance of the surface tensions (we are assuming that all GBs are isotropic, and we do not make a distinction between the GB energy and GB stress or tension):

$$\frac{dL}{dt} = m\gamma\left[1 - 2\sin\left(\frac{\Delta\theta}{2}\right)\right], \tag{3}$$

where L is the distance from the center of the grain to the pore located at the triple junction, and m is the mobility of the pore. The migration of an equilibrium triple junction pore (i.e., a pore with three dihedral angles, ψ, determined by the condition of mechanical equilibrium at the triple line where the GB and two free surfaces meet) controlled by surface diffusion was considered by Spears and Evans [12] and later by Riedel and Svoboda [13]. Numerical analysis

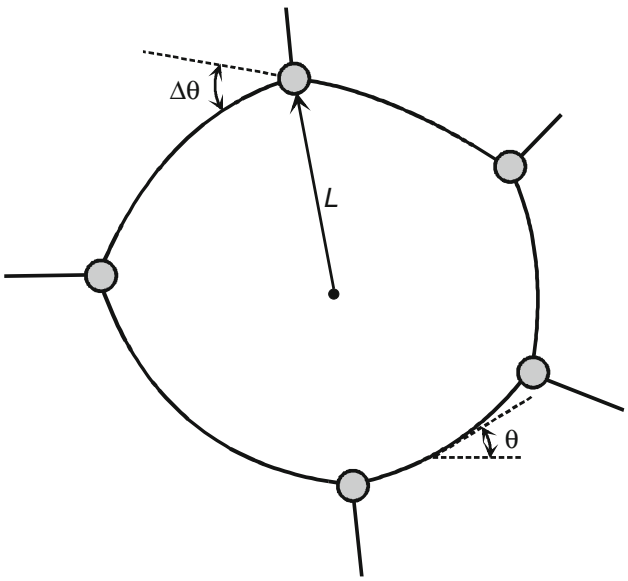

Fig. 1 Pores at triple junctions of a 5-sided grain of size L

of the governing diffusion equations showed that the migration rate depends on the angle ψ, and that at high migration rates the pore mobility becomes velocity-dependent [12]. For low pore migration rates Riedel and Svoboda derived the following velocity-independent expression for the pore mobility [13]:

$$m = \frac{\Omega D_s \delta}{\pi k T r^3} p(\psi), \tag{4}$$

where Ω, D_s, and δ are the atomic volume, surface diffusion coefficient, and the effective width of the surface layer in which diffusion occurs, respectively; k is the Boltzmann constant, and T is the absolute temperature. For non-circular pores r is understood as "effective radius", i.e., the radius of a circular pore of the same area as a non-circular one. The dimensionless factor $p(\psi)$ is given in Eq. 12 of the work of Riedel and Svoboda [13]. The angle ψ depends on the ratio of GB and surface energies according to $\cos\psi = \gamma/2\gamma_s$. The calculations show that for γ/γ_s varying from 0 to 1 the corresponding p values change in the narrow range from 1 to 0.92. Therefore, the introduction of factor p is not warranted in view of the number of simplifying assumptions made in this work, and in what follows it will be neglected.

For pores of infinite mobility the surface tension should be balanced at the triple junction, which corresponds to $\Delta\theta = \pi/3$. In this case Eq. 2 reduces to the classical von Neumann–Mullins equation [11]. Let us now assume that for pores with finite mobility $\Delta\theta = \pi/3 - \varphi$, where $\varphi \ll \pi/3$. Substituting this expression in Eqs. 2 and 3 yields

$$\frac{dS}{dt} = \frac{M\gamma\pi}{3}(n-6) - M\gamma n\varphi \tag{5}$$

and

$$\frac{dL}{dt} = m\gamma\varphi\frac{\sqrt{3}}{2}. \tag{6}$$

We will further assume that the shape of the grains is self-similar, i.e., $S = aL^2$ for all grains in the polycrystal, where a is a shape coefficient ($a \approx \pi$). In this case

$$\frac{dS}{dt} = 2aL\frac{dL}{dt}. \tag{7}$$

Substituting Eqs. 4, 6, and 7 in Eq. 5 we get

$$\frac{dL}{dt} = \frac{(n-6)M\gamma\pi/6a}{L + Mn/ma\sqrt{3}} = \frac{M\gamma(n-6)\pi/6a}{L + r^3\pi kTMn/\Omega D_s\delta a\sqrt{3}},$$

or, assuming for the sake of simplicity $a = \pi$,

$$\frac{dL}{dt} = \frac{M\gamma(n-6)/6}{L + r^3 kTM/\Omega D_s\delta n\sqrt{3}} \tag{8}$$

Eq. 8 shows that, similarly to the case of an ideal two-dimensional polycrystal, grains with $n > 6$ will grow and those with $n < 6$ will disappear in the course of grain growth. However, contrary to the classical Von Neumann–Mullins equation, the rate of grain growth/shrinkage is now dependent on the parameters of the pores (the second term in the denominator of Eq. 8). It should be noted that our Eq. 8 is similar to the Eq. 23 of the work of Riedel and Svoboda obtained using energy dissipation arguments [13]. Though Eq. 8 was derived for an individual grain with n sides, in what follows we will understand this equation in terms of the average grain size in a polycrystal and the average number of grain sides for all grains in a polycrystal, $\bar{n}$. This interpretation of Eq. 8 is similar in its spirit to the Burke–Turnbull model of normal grain growth (mean field approximation) [14].

Kinetics of grain growth with growing/shrinking pores

Following the approach of Yan, Cannon, and Chowdhry [6] we will represent the instantaneous rate of change of the pore radius as a sum of two contributions:

$$\frac{dr^3}{dt} = \left(\frac{dr^3}{dt}\right)_P + \left(\frac{dr^3}{dt}\right)_G \tag{9}$$

where the first term on the right-hand side (RHS) describes the increase of pore size due to the decrease of the number of triple junctions in the course of grain growth, and the second term gives the rate of shrinkage at constant grain size due to GB diffusion (see Fig. 2). The first term on the RHS of Eq. 9 can be found from the condition of a constant total pore area per unit area of the sample. Taking into consideration that there are $n/3$ pores per grain with n sides,

$$\frac{n}{3}\frac{\pi r^2}{aL^2} = const, \text{ and thus } \left(\frac{dr^3}{dt}\right)_P = 3\frac{r^3}{L}\frac{dL}{dt}. \tag{10}$$

Substituting Eqs. 8, 10, and the expression for the rate of pore shrinkage due to GB diffusion (see Appendix) in Eq. 9 we obtain

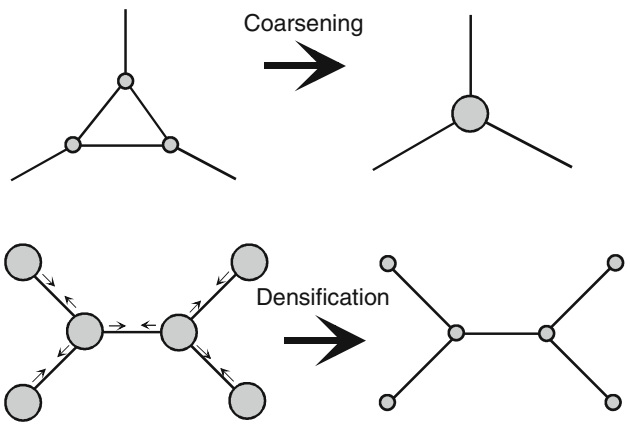

Fig. 2 Sketches of pore coarsening due to grain growth and densification due to grain boundary diffusion. The arrows in the sketch at the lower left-hand side denote the directions of vacancy flux

$$\frac{dr^3}{dt} = -\frac{27\overline{n}D_{GB}\delta\gamma_s\Omega}{4\pi^2 kT}\frac{1}{L} + \frac{M\gamma(\overline{n}-6)/6}{L + r^3 kTM/\Omega D_s\delta\overline{n}\sqrt{3}}\frac{3r^3}{L}. \quad (11)$$

Introducing dimensionless variables for the relative grain and pore size, and time

$$X = L/L_0, Y = (r/r_0)^3, \tau = tM\gamma(\overline{n}-6)/6L_0^2,$$

where L_0 and r_0 are initial grain and pore size, respectively, transforms Eqs. 8 and 11 to

$$\frac{dX}{d\tau} = \frac{1}{X+\alpha Y} \quad (12)$$

$$\frac{dY}{d\tau} = -\frac{\beta}{\alpha X} + \frac{3Y}{X(X+\alpha Y)}, \quad (13)$$

where

$$\alpha = \frac{r_0^3 kTM}{L_0\Omega D_s\delta}\frac{1}{\sqrt{3}\overline{n}} \quad (14)$$

$$\beta = \frac{D_{GB}\gamma_s}{D_s\gamma}\frac{81}{2\sqrt{3}\pi^2(\overline{n}-6)}. \quad (15)$$

Dividing both sides of Eq. 13 by the respective sides of Eq. 12 leads to the following equation:

$$\frac{dY}{dX} = -\frac{\beta}{\alpha} + (3-\beta)\frac{Y}{X} \quad (16)$$

which, taking into account the initial condition $Y(1) = 1$, can be easily solved:

$$Y = \frac{\beta}{\alpha(2-\beta)}X + \frac{2\alpha-\beta(1+\alpha)}{\alpha(2-\beta)}\cdot X^{(3-\beta)}. \quad (17)$$

The analysis of Eq. 17 shows that for $\beta < \beta_c$, where

$$\beta_c = \frac{2\alpha}{1+\alpha} \quad (18)$$

the relative pore size Y grows without limits with increasing X (and, hence, with increasing time). This means that in this case the grain growth prevents full densification of the nanocrystalline material which retains some porosity in spite of the fact that the pores reside at the triple junctions of the GBs. For $\beta > \beta_c$, Y drops to zero with increasing X, either monotonously or after achieving a maximum. The pores vanish at

$$X_{Y\to 0} \equiv X_0 = \left(\frac{\beta}{\beta(1+\alpha)-2\alpha}\right)^{1/(2-\beta)}. \quad (19)$$

Substituting Eq. 17 in Eq. 12 yields a time dependence of X for $Y > 0$:

$$\tau = \int_1^X dx(x+\alpha Y(x)) = -\frac{2+\alpha}{4-\beta} + \frac{1}{2-\beta}X^2 + \frac{2\alpha-\beta(1+\alpha)}{(4-\beta)(2-\beta)}X^{(4-\beta)} \quad (20)$$

and

$$\tau_{Y\to 0} = \frac{1}{4-\beta}\left[2\left(\frac{\beta}{\beta(1+\alpha)-2\alpha}\right)^{2/(2-\beta)} - 2 - \alpha\right]. \quad (21)$$

It follows from Eq. 12 that for $\beta > \beta_c$ the grain growth becomes parabolic for $\tau > \tau_{Y\to 0}$, i.e., after full densification is achieved. The unified $X(\tau)$ dependence for all τ can be obtained in this case by combining Eq. 12 with Eqs. 19 and 20:

$$\tau(X) = \begin{cases} -\frac{2+\alpha}{4-\beta} + \frac{X^2}{2-\beta} - \frac{\beta X^2}{(2-\beta)(4-\beta)}\left(\frac{X}{X_0}\right)^{2-\beta} & X < X_0 \\ -\frac{2+\alpha}{4-\beta} + \frac{\beta X_0^2}{2(4-\beta)} + \frac{X^2}{2} & X > X_0 \end{cases} \quad (22)$$

Eqs. 19–22 represent the main result of this work.

Discussion

The temporal behavior of a polycrystal with pores is determined by the dimensionless parameters α and β given by Eqs. 14 and 15. However, trying to estimate these parameters for any specific material is difficult, if not impossible, since the kinetic coefficients D_{GB}, D_s and M in these equations depend sensitively on the impurity content of the material, annealing conditions, and many other factors that may change them by orders of magnitude. To the best of our knowledge, no self-consistent set of GB diffusivities, GB mobilities, and surface diffusivities in a material of well-defined chemical composition under well-defined annealing conditions is available in the literature. We will follow the approach of Mishin, Kaur, and Gust and instead of making estimates for a specific material consider a "typical" face centered cubic (fcc) metal [15]. According to a compilation of Ref. [15],

$$\delta D_{GB} = 9.7\times 10^{-15}\exp\left(-9.07\frac{T_m}{T}\right)\mathrm{m}^3/\mathrm{s} \quad (23a)$$

and

$$\delta D_s = 7.8\times 10^{-16}\exp\left(-6.55\frac{T_m}{T}\right)\mathrm{m}^3/\mathrm{s}, \quad (23b)$$

where we assumed for simplicity that the thickness of diffusion layers is the same for GBs and surfaces. Though it is known that different atomic jumps are responsible for GB migration and GB diffusion [16], we will use a rough estimate suggested by Sinclair, Hutchinson and Brechet for the GB mobility in pure material [17]:

$$M = B\frac{\delta D_{GB}\Omega}{b^2 kT} \quad (24)$$

where B is a numerical coefficient close to one and b is the magnitude of the Burgers vector. In Ref. [17] it was found that $B \approx 0.7$ for pure iron. For estimating the average

number of grain sides, $\overline{n}$, we note that computer simulations of two-dimensional grain growth yielded $d\overline{S}/dt \approx 1.8M\gamma$ for the growth rate of the average grain area, $\overline{S}$ [18]. Comparing this result with the von Neumann–Mullins relationship in which the area and the number of sides of the individual grains are replaced by respective average values for a polycrystal gives $\overline{n} \approx 7.7$. We will further assume that $\gamma_s/\gamma \approx 3$, which is a typical ratio of surface and GB energies in pure metals [14]. Assigning $L_0 = 20$ nm and $r_0 = 2$ nm as characteristic values for the initial grain and pore sizes in a nanocrystalline material yields the following expressions for the temperature-dependent parameters α and β:

$$\alpha \approx 4.2 \times \exp\left(-2.52\frac{T_m}{T}\right) \text{ and}$$
$$\beta \approx 52.0 \times \exp\left(-2.52\frac{T_m}{T}\right) \quad (25)$$

The values of α and β for several homologous temperatures relevant for grain growth in nanocrystalline materials are presented in Table 1. It can be seen from this table that $\alpha \ll 1$ for low temperatures and, hence, the condition (18) can be re-written in the form $\beta_c = 2\alpha$. Following the analysis of the previous Section, and using the definitions of the parameters α and β in Eqs. 14 and 15 we arrive at the conclusion that a nanocrystalline material with initial pore size larger than r_0^*, where

$$\left(r_0^*\right)^3 \approx \frac{81\gamma_s\overline{n}b^2}{4\pi^2 B\gamma(\overline{n}-6)}L_0, \quad (26)$$

cannot achieve full density during grain growth, i.e., the pores will grow without limits with increasing grain size. In this case, and for long annealing times, the last term on the RHS of Eq. 20 will dominate, and the grain growth law can be written in the following form:

$$\left(\frac{L}{L_0}\right)^{4-\beta} \approx \frac{(4-\beta)(2-\beta)}{2\alpha-\beta(1+\alpha)}\frac{M\gamma(\overline{n}-6)}{6L_0^2}t \quad (27)$$

For $\beta \ll 1$, Eq. 27 can be reduced to the result of Brook [Eq. 1] that disregards sintering during grain growth. In the general case in which sintering cannot be disregarded the grain growth exponent can vary continuously from 2 to 4, depending on the relation among the various kinetic parameters of the system (it should be noted that according to Eq. 18 $0 < \beta_c < 2$). To our knowledge, this is the first analytical model of grain growth that predicts a continuous spectrum of the growth exponent from 2 to 4. It should be noted that grain growth exponents higher than two are often observed in experiments [14].

Using Eq. 26 and assuming $b = 0.25$ nm, $L_0 = 50$ nm we arrive at a critical pore size of $r_0^* \approx 5$ nm. Polycrystals with pores of larger initial dimensions will exhibit grain growth behavior very different from their counterparts with smaller pores: while in the former the pores will grow without limits with increasing grain size, in the latter the pores will eventually disappear and the nanocrystalline material will attain full density.

Figure 3 is an example of the grain and pore growth kinetics in a system with subcritical initial pore size ($r_0 < r_0^*$). The initial part of the $X(\tau)$ dependence can be fairly well approximated by a linear function. This type of linear growth law followed by a parabolic one was observed by Cao and Zhang during grain growth in thin nanocrystalline Cu films (see Fig. 3 in Ref. [19]), and by Krill and co-workers during grain growth in bulk nanocrystalline iron (see Fig. 1 in Ref. [20]). Since such linear growth law is often considered as a typical feature of the initial stages of grain growth in nanocrystalline materials [8, 9, 20], we analyzed where in the parametric (α,β) plane one has to expect a linear growth law in the framework of our model. Let us consider a linear approximation of Eq. 22:

$$\tilde{\tau}(X) = \eta \cdot (X-1), \text{ for } 1 < X < X_m, \text{ where}$$
$$X_m = \begin{cases} X_0 & X_0 > 2 \\ 2 & X_0 < 2 \end{cases} \quad (28)$$

Obviously, the linear growth law is associated with the effect of triple junction pores on grain growth and,

Table 1 Parameters α and β (see Eqs. 14, 15) for a typical fcc metal (according to correlations of Mishin et al. [15]) at different homologous temperatures

T/T_m	0.2	0.3	0.4	0.5
α	1.4×10^{-5}	9.4×10^{-4}	7.8×10^{-3}	0.028
β	1.8×10^{-4}	1.2×10^{-2}	9.6×10^{-2}	0.34

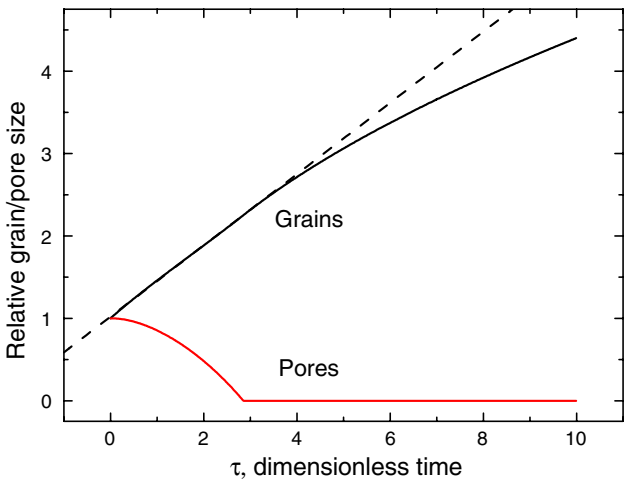

Fig. 3 Kinetics of grain growth and pore shrinkage for $\alpha = 1$ and $\beta = 1.5$ (see Eqs. 14, 15 for definitions). Pore-controlled linear growth is followed by parabolic growth after the pores disappear

therefore, a linear interpolation of the $X(\tau)$ dependence makes sense for $X < X_0$. However, for X_0 which is too close to 1 the linear interpolation will always work just because of $X - 1$ being small in the interval $1 < X < X_0$. To exclude this "artificial" linearization from our analysis we selected (somewhat arbitrarily) $X = 2$ as a lower limit for the range of grain sizes to be linearized.

The least square analysis of the linear interpolation (28) of Eq. 22 yields:

$$\eta = \frac{3}{(X_m - 1)^3} \int_1^{X_m} (X - 1)\tau(X)dX \tag{29}$$

and

$$\rho^2 \equiv \frac{1}{X_m - 1} \int_1^{X_m} [\tau(X) - \tilde{\tau}(X)]^2 dX = \frac{1}{X_m - 1} \int_1^{X_m} \tau^2(X)dX - \frac{\eta^2}{3}(X_m - 1)^2, \tag{30}$$

where ρ is an average error associated with the linear interpolation. For the linear approximation to be of a high accuracy, the inequality $\rho \ll \tau_{Y\to 0}$ has to be fulfilled. Figure 4 shows the borders of the two regions in the parametric (α, β) plane which are defined by the inequalities $\rho < 0.01\tau_{Y\to 0}$ and $\rho < 0.02\tau_{Y\to 0}$. Both regions are located above the dashed line defined by Eq. 18: this line separates the region in which pores at triple junctions grow without limits with increasing time (below the line) from the region in which pores vanish with time (above the line). The set of parameters employed in calculating the $X(\tau)$ and $Y(\tau)$ dependencies shown in Fig. 3 ($\alpha = 1$, $\beta = 1.5$) is within the region defined by the stricter of the two inequalities. The good quality of a linear fit for $X(\tau)$ is clearly visible in this figure.

An example of the time dependence of the grain and pore size for parameters α and β which are outside the linearization regions defined in Fig. 4 is shown in Fig. 5. A sigmoidal shape of the $X(\tau)$ curve with an "incubation time" during which grain growth is particularly slow is clearly discernible in this figure. A similar phenomenon of stabilization of the nanocrystalline microstructure was predicted in the model in which migrating GBs eject their free volume into the bulk in the course of grain growth [21].

We expect that, qualitatively, the kinetic behavior of three-dimensional polycrystals with cylindrical pores at the GB triple junctions will be similar to the behavior of the 2D polycrystal considered in the present work. This follows from the similarity of our Eq. 8 and kinetic equation of Riedel and Svoboda describing the grain growth in the three-dimensional case [13]. Moreover, there is a topological similarity of the problem of circular pore dissolution in the 2D case and a corresponding three-dimensional problem of the dissolution of a cylindrical pore located at the triple line (see Appendix). However, the kinetics of shrinkage of the isolated pores at the grain corners of a three-dimensional polycrystal may be very different from the one considered in the present work. Indeed, our preliminary calculations show that for isolated pores located at the grain corners the dependence of the shrinkage rate on grain size is much weaker (logarithmic) than for cylindrical pores at the triple lines. This may enable full densification for all initial conditions. A detailed analysis of the three-dimensional problem will be given elsewhere [22].

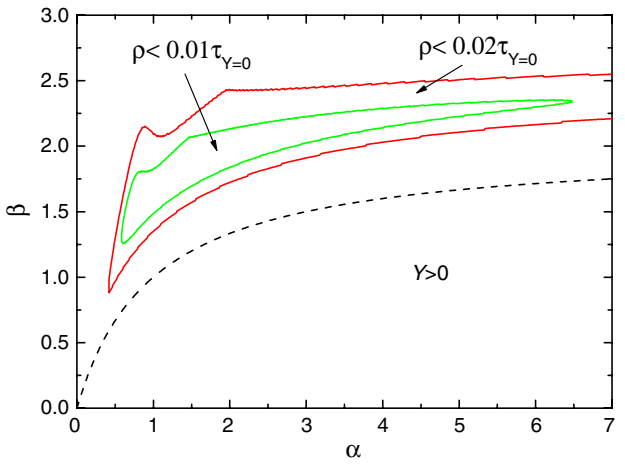

Fig. 4 Regions of good linerarization of the $X(\tau)$ dependence at the initial stages of grain growth. Smaller region (bounded by a green line in the on-line version of this paper) corresponds to a stricter linearization criterion

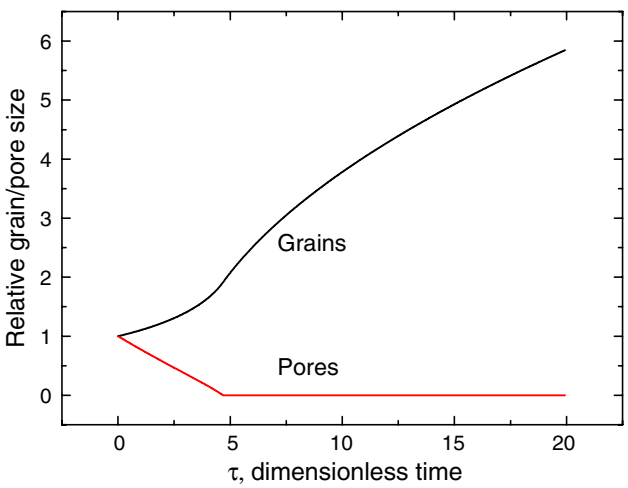

Fig. 5 Kinetics of grain growth and pore shrinkage for $\alpha = 10$ and $\beta = 5$. Pores slow down the grain growth at the initial stages of the process

Conclusions

We considered grain growth in a two-dimensional nanoscale polycrystal with small mobile pores located at the GB triple junctions. A model describing grain growth in such porous nanocrystalline material that proceeds simultaneously with densification controlled by GB diffusion was developed. The following conclusions can be drawn from the present study:

1. The grain growth behavior crucially depends on the initial pore size. A unique critical value of the initial pore size can be calculated for each combination of GB and surface diffusivities and energies, GB mobility and initial grain size. The subcritical pores disappear from the system in the course of grain growth, whereas the supercritical pores grow without limits with the growing grains, so that densification cannot be completed.
2. For a supercritical initial pore size grain growth at long annealing times follows a power law, with a growth exponent anywhere between 2 and 4 depending on the relevant kinetic parameters.
3. For a subcritical initial pore size a linear growth law can be observed at the initial stages of grain growth. After the pores disappear the grain growth becomes parabolic. Such linear grain growth followed by a parabolic one was recently observed in thin Cu films [19] and bulk nanocrystalline Fe [20].

Acknowledgements This work was supported by the Russell Berrie Nanotechnology Institute (Technion) and by the RWTH Aachen through the Umbrella Cooperation Program.

Appendix

Dissolution of a circular pore at a triple junction

Let us consider a cylindrical pore of radius r located at a GB triple junction in a two-dimensional polycrystal. We will assume that pore dissolution is controlled by GB diffusion alone. The diffusion flux, j, along the GB (per unit length of the pore) is

$$j = -\frac{D_{GB}\delta}{kT}\frac{\partial \sigma_{nn}}{\partial x}, \tag{A1}$$

where σ_{nn} is the normal stress at the GB, and x is the coordinate along the GB. D_{GB} is the GB-self diffusion coefficient and we assume for simplicity that the diffusional width of the GB is equal to that of the surface. In the middle between two identical pores ($x = 0$) this flux should vanish because of symmetry reasons. In the steady state sintering regime the drift velocities of two grains normal to the GB should be constant, which means that the divergence of the flux j given by Eq. A1 is also constant. In this case

$$\sigma_{nn}(x) = ax^2 + b, \tag{A2}$$

where a and b are constants. The distance between neighboring pores is $2l \approx 2\pi L/n - 2r$ (see Fig. 1). The chemical potential of the atoms on the pore surface and at the triple junction between the pore surface and a GB are $\mu_0 - \gamma_s\Omega/r$ and $\mu_0 + \sigma_{nn}\Omega$, respectively (here, γ_s is the surface energy and μ_0 is the chemical potential of atoms in the crystal bulk). From the balance of these chemical potentials we get

$$\sigma_{nn}|_{x=l} = -\gamma_s/r. \tag{A3}$$

To find the unknown constants a and b we use the boundary condition A3 and the total force balance at the GB:

$$-\gamma_s + \int_0^l \sigma_{nn}(x)dx = 0, \tag{A4}$$

which yields $a = -\frac{3\gamma_s(l+r)}{2rl^3}$. For the atomic flux to the pore we obtain from Eqs. A1 and A2

$$j_{x=l} = \frac{3\gamma_s D_{GB}\delta}{2kT}\frac{l+r}{rl^2}. \tag{A5}$$

The rate of pore dissolution can be found from the condition of mass balance:

$$2\pi r\frac{dr}{dt} = -3\Omega j|_{x=l} \tag{A6}$$

$$\frac{dr}{dt} = -\frac{9D_{GB}\delta\gamma_s\Omega}{4\pi kT}\frac{l+r}{r^2l^2}. \tag{A7}$$

For $l \gg r$

$$\frac{d(r^3)}{dt} = -\frac{27D_{GB}\delta\gamma_s\Omega}{4\pi kT}\frac{1}{l} \approx -\frac{27nD_{GB}\delta\gamma_s\Omega}{4\pi^2 kT}\frac{1}{L}.$$

References

1. Gleiter H (1989) Prog Mater Sci 33:223. doi:10.1016/0079-6425(89)90001-7
2. Chaudhari PJ (1972) Vac Sci Technol 9:520. doi:10.1116/1.1316674
3. Upmanyu M, Srolovitz DJ, Gottstein G, Shvindlerman LS (1998) Interface Sci 6:289. doi:10.1023/A:1008653704896
4. Shvindlerman LS, Gottstein G, Ivanov VA, Molodov DA, Kolesnikov D, Lojkowski W (2006) J Mater Sci 41:7725. doi:10.1007/s10853-006-0563-0
5. Brook RJ (1976) In: Wang FFY (eds) Treatise on materials science and technology, vol 9. Academic, New York, pp 331–363
6. Yan MF, Cannon RM, Chowdhry U (1978) Am Ceram Bull 57:316
7. Gottstein G, Shvindlerman LS (1993) Acta metal mater 41:3267
8. Gottstein G, Ma Y, Shvindlerman LS (2005) Acta mater 53:1535. doi:10.1016/j.actamat.2004.12.006
9. Gottstein G, Shvindlerman LS (2006) Scripta mater 54:1065. doi:10.1016/j.scriptamat.2005.11.057

10. Cahn JW (1962) Acta metal 10:789
11. Gottstein G, Shvindlerman LS (1999) Grain boundary migration in metals. CRC Press, Boca Raton
12. Spears MA, Evans AG (1982) Acta metal 30:1281
13. Riedel H, Svoboda J (1993) Acta metal mater 41:1929
14. Humphreys FJ, Hatherly M (1996) Recrystallization and related annealing phenomena. Elsevier, Oxford
15. Mishin Y, Kaur I, Gust W (1995) Fundamentals of grain and interphase boundary diffusion. Wiley, Chichester
16. Schönfelder B, Gottstein G, Shvindlerman LS (2005) Acta mater 53:1597. doi:10.1016/j.actamat.2004.12.010
17. Sinclair CW, Hutchinson CR, Brechet Y (2007) Met Mater Trans A 38:821. doi:10.1007/s11661-007-9106-9
18. Fradkov VE, Udler D (1994) Adv Phys 43:739. doi:10.1080/00018739400101559
19. Cao P, Zhang B (2006) Int J Mod Phys B 20:3830. doi:10.1142/S0217979206040441
20. Krill III CE, Helfen L, Michels D, Natter H, Fitch A, Masson O, Birringer R (2001) Phys Rev Lett 86:842. doi:10.1103/PhysRevLett.86.842
21. Estrin Y, Gottstein G, Rabkin E, Shvindlerman LS (2000) Scripta mater 43:141. doi:10.1016/S1359-6462(00)00383-3
22. Klinger L, Rabkin E, Shvindlerman LS, Gottstein G (2008) J Mater Sci, to be submitted